****
****

Document-ID: 382523

Patron:

Note:

NOTICE:

****
****

Pages: 9 Printed: 03-10-04 13:01:13

Sender: Ariel/Windows

Journal Title: Journal of the Acoustical Society of America

Volume: 60
Issue: 1
Month/Year: 1976
Pages: 2--8

Article Author: Yew, C.H. and Yogi, P.N.

Article Title: Study of wave motion in fluid-saturated porous rocks

Study of wave motions in fluid-saturated porous rocks*

C. H. Yew and P. N. Jogi

Department of Aerospace Engineering and Engineering Mechanics, The University of Texas at Austin, Austin, Texas 78712

(Received 5 November 1975; revised 25 March 1976)

In this investigation, Biot's theory was employed in the study of wave motions in fluid-saturated porous rocks. Consistent with the described experimental arrangement, Biot's equations were solved using a Laplace transformation. The theory predicts two dilatational waves: a slightly dispersed fast wave propagating ahead of a heavily dispersed and attenuated slow wave. By comparing these results with experimental results, it becomes evident that the measured waves are in fact the fast waves.

Subject Classification: [43] 20.15, [43] 20.40; [43] 40.50.

INTRODUCTION

A porous material may be regarded as a material whose solid portion is continuously connected throughout the whole volume to form a loosely connected solid matrix and voids through which the fluid or gas may flow. The importance in understanding the propagation of stress waves in such a medium to petroleum engineers and the geologists need not be emphasized here. Extensive research in this subject has been carried out by many authors,[1–5] and different theories regarding the wave propagation in such a medium have been developed. One of the well established theories is due to Biot.[6,7] In his approach, the macroscopic stress–strain relation of a fluid-saturated porous medium was derived by assuming the existence of a strain-energy density function; the coupling effect between the solid skeleton and the contained fluid was taken into consideration by introducing a mass (inertia) coupling parameter into the kinetic energy of the system; and the damping effect of the contained fluid was expressed by dissipation energy expressed in terms of the relative velocity between the fluid and the solid. Using Lagrangian equations, Biot derived the equations of motion for this system which for a one-dimensional case has the form

$$\begin{aligned} P\frac{\partial^2 u}{\partial x^2}+Q\frac{\partial^2 U}{\partial x^2}&=\rho_{11}\frac{\partial^2 u}{\partial t^2}+\rho_{12}\frac{\partial^2 U}{\partial t^2}+b\frac{\partial}{\partial t}(u-U)\\ Q\frac{\partial^2 u}{\partial x^2}+R\frac{\partial^2 U}{\partial x^2}&=\rho_{12}\frac{\partial^2 u}{\partial t^2}+\rho_{22}\frac{\partial^2 U}{\partial t^2}-b\frac{\partial}{\partial t}(u-U), \end{aligned} \tag{1}$$

where u is the displacement of the solid skeleton and U is the displacement of the fluid. The parameters P, Q, and R represent the mechanical properties of the fluid-saturated porous medium. A detailed discussion of these parameters was made by Biot and Willis.[8] These parameters are inherently positive and satisfy the inequality

$$PR-Q^2>0. \tag{2}$$

The parameters ρ_{11}, ρ_{22}, and ρ_{12} are the dynamic coefficients that take into account the inertia effect of the moving fluid. These parameters are related to mass densities of the solid (ρ_s) and the fluid (ρ_f) by the equations

$$\begin{aligned} \rho_{11}+\rho_{12}&=(1-\beta)\rho_s\ ,\\ \rho_{12}+\rho_{22}&=\beta\rho_f \end{aligned} \tag{3}$$

and satisfy the inequalities

$$\begin{aligned} &\rho_{11}>0,\ \rho_{22}>0,\ \ \rho_{12}<0,\\ &\rho_{11}\rho_{22}-\rho_{12}^2>0,\\ &P\rho_{22}+R\rho_{11}-2Q\rho_{12}>0, \end{aligned} \tag{4}$$

where β is the porosity of the medium and ρ_{12} is the coupling parameter. The physical significance of these parameters has been discussed by Biot[6] and will not be repeated here.

Finally, the parameter b represents the damping coefficient between the fluid and the solid. In analogy to Darcy's equation, coefficient b may be related to the permeability K, the porosity β, and the fluid viscosity μ by the equation

$$b=\mu\beta^2/K. \tag{5}$$

Realizing that the viscosity μ may be dependent on the frequency and geometry of the pores, a method for correction of μ was also developed by Biot.[7]

Biot's theory predicts the existence of two attenuated dilatational waves (P_f and P_s) and one attenuated rotational wave (S). Using Biot's equation, the problems of the reflection and refraction of waves at the interface, and the surface waves in such a medium were extensively studied by Jones,[9] Deresiewicz,[10–13] and Geertsma and Smit.[14]

The experimental investigations on the wave motions in a fluid-saturated porous medium do not, however, match the above quoted analytical development. Although the sonic-pulse technique has been extensively used in determining the well characteristics[15] and the rock properties,[16–18] the theoretical foundation of this technique is based on the consideration of elastic waves in an elastic anisotropic medium. A qualitative application of Biot's theory in the interpretation of experimental results, to the best of author's knowledge, is scarce. Using the sonic pulse technique a great amount of data on the wave speeds in the fluid-saturated rocks of various porosities and confining pressures were obtained by Fatt,[9] Wyllie, Gregory, and Gardner[20,21] and Gregory.[22] The purpose of this study is to make a comparative study of these experimental results with that predicted by Biot's theory.

In the following sections, Eq. (1), is solved consis-

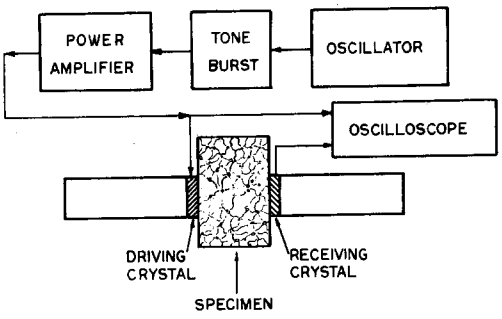

FIG. 1. Experimental arrangement.

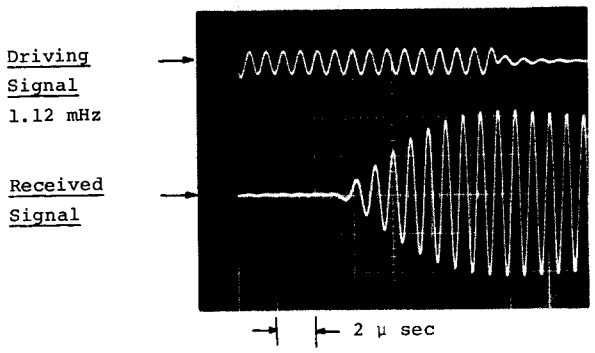

FIG. 2. A typical oscilloscope record for water-saturated dolomite (Kasota): $B=0.108$; thickness = 1 in.: tested at atmospheric pressure.

tent with the experimental arrangement and the characteristics of waves are discussed in detail. The results are then discussed and compared with Fatt's and Gregory's data.

I. ANALYSIS

The experimental arrangement for obtaining the rock properties using the sonic pulse technique is sketched in Fig. 1.[17] The fluid-saturated porous specimen is sandwiched between a pair of resonant-frequency-matched piezoelectric crystal disks. One of the piezoelectric disks serves as the driver and the other serves as the receiver. A train of oscillations, either at a single frequency or in the form of a wide-band pulse, is tone bursted into the specimen by the driving disk. The signal which propagates through the specimen, is monitored by the receiving crystal. The wave speed is then obtained by dividing the specimen thickness by the measured transit time. A typical oscilloscope record from the test is shown in Fig. 2. The detailed experimental arrangement and technique is described in Refs. 17 and 23 and will not be repeated here.

Consistent with the above-described experimental arrangement and method, the boundary conditions for Eq. (1) may be written as

$$u(0,t)=U(0,t)=U_{1n}\sin\omega t[H(t)-H(t-T)], \tag{6}$$

where U_{1n} is the amplitude of oscillation, $H(t)$ is the Heaviside step function, ω is the angular frequency of the oscillation, and T is the time period of the pulse.

Since the wave speed, or the arrival time of the wave, is of main concern in this experiment, it is reasonable to assume that the specimen is semi-infinite as long as the arrival of the waves is not affected by the reflected waves from the boundaries of the specimen. In the following analysis, we further assume that the output voltage of the receiving disk is directly proportional to the average displacement of the fluid and the solid portion of the specimen over the contact area of the disk, i.e.,

$$V_{out}=K_1[u(x,t)+U(x,t)], \tag{7}$$

where K_1 is the calibration constant. [The value of K_1, which depends on the strength of the signal, and relative stiffness between the crystal disk and specimen, is difficult to determine accurately.] Again, since the wave speed is of main concern here, the numerical value of constant K_1 is not important in the analysis.

Applying Laplace transformation to Eqs. (1) and (6) and assuming that the medium is initially at rest, the displacement $u(x,t)+U(x,t)$, after considerable algebraic manipulations, has the form

$$u+U=\frac{mU_{1n}\omega}{2\pi i}\left(\int_{Br}\frac{(1-e^{-Ts})[sa-f+(s^2+ds+f^2)^{1/2}][-sh+n+(s^2+ds+f^2)^{1/2}]}{(s^2+\omega^2)(s-\eta)(s^2+ds+f^2)^{1/2}}\right.$$

$$\left.\times\exp(-\lambda_1 x+st)\,ds+\int_{Br}\frac{(1-e^{-Ts})[sa-f-(s^2+ds+f^2)^{1/2}][sh-n+(s^2+ds+f^2)^{1/2}]}{(s^2+\omega^2)(s-\eta)(s^2+ds+f^2)^{1/2}}\exp(-\lambda_2 x+st)ds\right), \tag{8}$$

where λ_1 and λ_2 are the roots of equation

$$A\lambda^4-(Es+Bs^2)\lambda^2+(Cs^4+Ds^3)=0. \tag{9}$$

The constants in Eqs. (8) and (9), written in terms of Biot's constants, are defined as follows:

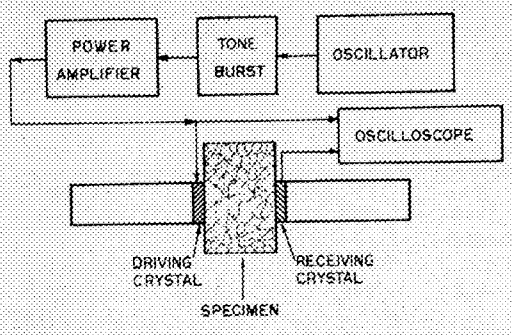

FIG. 1. Experimental arrangement.

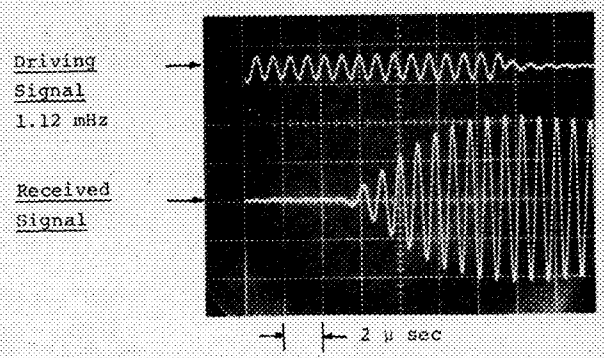

FIG. 2. A typical oscilloscope record for water-saturated dolomite (Kasota): $B=0.108$; thickness = 1 in.; tested at atmospheric pressure.

tent with the experimental arrangement and the characteristics of waves are discussed in detail. The results are then discussed and compared with Fatt's and Gregory's data.

I. ANALYSIS

The experimental arrangement for obtaining the rock properties using the sonic pulse technique is sketched in Fig. 1.[17] The fluid-saturated porous specimen is sandwiched between a pair of resonant-frequency-matched piezoelectric crystal disks. One of the piezoelectric disks serves as the driver and the other serves as the receiver. A train of oscillations, either at a single frequency or in the form of a wide-band pulse, is tone bursted into the specimen by the driving disk. The signal which propagates through the specimen, is monitored by the receiving crystal. The wave speed is then obtained by dividing the specimen thickness by the measured transit time. A typical oscilloscope record from the test is shown in Fig. 2. The detailed experimental arrangement and technique is described in Refs. 17 and 23 and will not be repeated here.

Consistent with the above-described experimental arrangement and method, the boundary conditions for Eq. (1) may be written as

$$u(0,t)=U(0,t)=U_{in}\sin\omega t\,[H(t)-H(t-T)], \tag{6}$$

where U_{in} is the amplitude of oscillation, $H(t)$ is the Heaviside step function, ω is the angular frequency of the oscillation, and T is the time period of the pulse.

Since the wave speed, or the arrival time of the wave, is of main concern in this experiment, it is reasonable to assume that the specimen is semi-infinite as long as the arrival of the waves is not affected by the reflected waves from the boundaries of the specimen. In the following analysis, we further assume that the output voltage of the receiving disk is directly proportional to the average displacement of the fluid and the solid portion of the specimen over the contact area of the disk, i.e.,

$$V_{out}=K_1[u(x,t)+U(x,t)], \tag{7}$$

where K_1 is the calibration constant. [The value of K_1, which depends on the strength of the signal, and relative stiffness between the crystal disk and specimen, is difficult to determine accurately.] Again, since the wave speed is of main concern here, the numerical value of constant K_1 is not important in the analysis.

Applying Laplace transformation to Eqs. (1) and (6) and assuming that the medium is initially at rest, the displacement $u(x,t)+U(x,t)$, after considerable algebraic manipulations, has the form

$$u+U=\frac{mU_{in}\omega}{2\pi i}\left(\int_{Br}\frac{(1-e^{-Ts})[sa-f+(s^2+ds+f^2)^{1/2}][-sh+n+(s^2+ds+f^2)^{1/2}]}{(s^2+\omega^2)(s-\eta)(s^2+ds+f^2)^{1/2}}\right.$$

$$\left.\times\exp(-\lambda_1 x+st)\,ds+\int_{Br}\frac{(1-e^{-Ts})[sa-f-(s^2+ds+f^2)^{1/2}][sh-n+(s^2+ds+f^2)^{1/2}]}{(s^2+\omega^2)(s-\eta)(s^2+ds+f^2)^{1/2}}\exp(-\lambda_2 x+st)ds\right), \tag{8}$$

where λ_1 and λ_2 are the roots of equation

$$A\lambda^4-(Es+Bs^2)\lambda^2+(Cs^4+Ds^3)=0. \tag{9}$$

The constants in Eqs. (8) and (9), written in terms of Biot's constants, are defined as follows:

$$A = PR - Q^2; \qquad d = \frac{2BE - 4DA}{B^2 - 4AC},$$

$$B = R\rho_{11} + P\rho_{22} - 2Q\rho_{12}, \qquad f = \frac{E}{(B^2 - 4AC)^{1/2}},$$

$$C = \rho_{11}\rho_{22} - \rho_{12}^2; \qquad h = \frac{(R(\rho_{11} - 2\rho_{12}) - (P - 2Q)\rho_{22}}{(B^2 - 4AC)^{1/2}},$$

$$D = b(\rho_{11} + \rho_{22} + 2\rho_{12}), \qquad m = \frac{(B^2 - 4AC)^{1/2}}{4(R\rho_{12} - Q\rho_{22})}, \tag{10}$$

$$E = (P + R + 2Q)\, b, \qquad n = \frac{(P - 2Q - 3R)\, b}{(B^2 - 4AC)^{1/2}},$$

$$a = \frac{R(\rho_{11} + 2\rho_{12}) - (P + 2Q)\rho_{22}}{(B^2 - 4AC)^{1/2}}, \qquad \eta = \frac{(R + Q)b}{R\rho_{12} - Q\rho_{22}}.$$

We note that Eq. (9) becomes the dispersion equation for dilatational waves derived by Deresiewicz[10] when the Laplacian parameter s is replaced by $i\omega$. Equation (8) obviously suggests the existence of two dilatational waves in accordance with parameters λ_1 and λ_2. It should be mentioned here that the nature of the integral in Eq. (8) is very similar to the integral obtained in the study of wave motions in fiber reinforced composites.[24] A representative contour for evaluating the integrals in Eq. (8) is shown in Fig. 3. By evaluating the contour enclosed by the large semicircle on the right half plane and making use of Jordan's lemma, the propagation speeds of the two waves may be expressed as

$$V_{1,2}^2 = \left[\frac{2(PR - Q^2)}{(R\rho_{11} + P\rho_{22} - 2Q\rho_{12}) \mp [(R\rho_{11} + P\rho_{22} - 2Q\rho_{12})^2 - 4(PR - Q^2)(\rho_{11}\rho_{22} - \rho_{12}^2)]^{1/2}}\right]. \tag{11}$$

Equation (11) has the same form as that obtained by Biot[6] and Deresiewicz.[10] Following Biot,[6] V_1 and V_2 are denoted respectively as the fast wave v_f and slow wave v_s.

In the following discussions, the integral in Eq. (8) is evaluated numerically based on the material properties of kerosene-saturated[19] and water-saturated sandstones.[22] The material properties and the corresponding Biot's coefficients are tabulated in Table I. Referring to Fig. 3, the poles, $s = \pm i\omega$, contribute the steady-state solution of Eq. (8). After considerable computations, the results may be summarized as follows: Corresponding to λ_1 and λ_2, the two waves with propagation speeds v_f and v_s have the form

$$u + U = A_l \exp[ik_x(x - c_l t)], \tag{12}$$

where $l = 1, 2$ relates the corresponding contributions from the parameters λ_1 and λ_2. The plot of k_l with c_l provides the information on the dispersive characteristics of waves in the medium. Figures 4 and 5 show the dispersion curves of the fast and slow waves in the kerosene- and water-saturated sandstones at various damping coefficients respectively. The amplitude A_l of waves of both kinds are not only frequency dependent but also spacially (distance) dependent. Figures 6–9 show such dependencies with damping factors $b = 1$ and 12 for both sandstones.

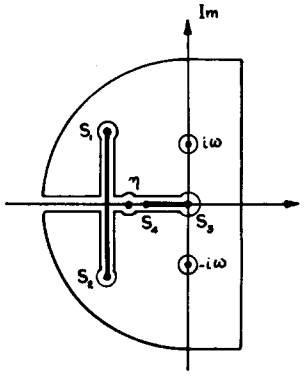

FIG. 3. Contour of integration.

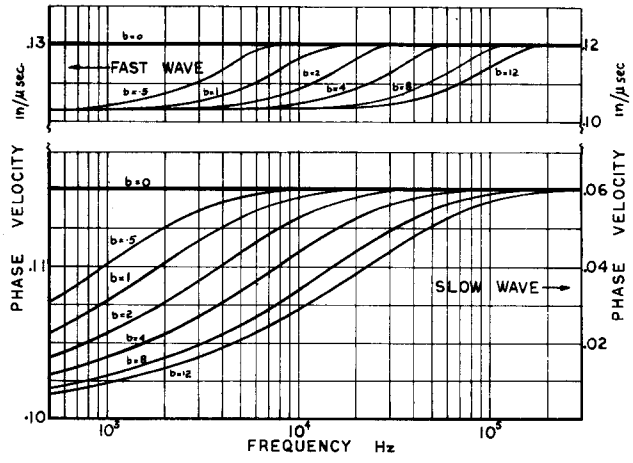

FIG. 4. Dispersion curves of waves in water-saturated Boise sandstone.

TABLE I. Material constants and wave speeds.

Material	Fluid	Pressure (psi)	Compressibility of fluid[a] $\times 10^{-6}$ lb/in.^{2}	Porosity β	Bulk Density $\times 10^{-4}$ lb sec^2/ in.^{4}	Biot–Willis Constants $\times 10^6$ psi P	R	Q
Limestone (Indiana)	Water	10 000	2.0 (assumed)	0.173	2.248	5.654	0.0849	0.0118
Dolomite (Kasota)	Water	5 000	2.8	0.108	2.449	8.622	0.0381	0.0063
Limestone (Indiana)	Water	5 000	2.8	0.144	2.295	5.632	0.0483	0.0386
Limestone (Indiana)	Water	5 000	2.8	0.173	2.245	5.096	0.0584	0.0315
Sandstone (Beria)	Water	5 000	2.8	0.207	2.164	4.568	0.0718	0.0159
Sandstone (Boise)	Water	5 000	2.8	0.268	2.045	3.118	0.0923	0.0188
Limestone (Indiana)	Water	1 000	3.3	0.173	2.242	3.579	0.0454	0.0600
Sandstone (Boise)	Water	1 000	3.3	0.268	2.041	2.666	0.0745	0.0450
Chalk	Water	1 000	3.3	0.306	2.029	1.982	0.0828	0.0548
Chalk	Water	1 000	3.3	0.388	1.882	1.266	0.1153	0.0183
Sandstone[b] (Boise)	Kerosene	5 000	5.0	0.260	2.446	1.445	0.0473	0.1078

Material	Calculated Velocity from Eq. (11) $\rho_{12}=0$ (ft/sec) v_f	v_s	Calculated Velocity from Eqs. (16) and (17) (ft/sec) v_f	v_s	Measured Velocities (ft/sec) Dry Specimen 0% Saturation	Wet Specimen 100% Saturation	Calculated ρ_{12} $\times 10^{-6}$
Limestone (Indiana)	13 721	6 018	13 721	6 018	13 670	14 085	0.61
Dolomite (Kasota)	15 970	5 108	15 971	5 103	16 340	16 340	4.87
Limestone (Indiana)	13 466	4 946	13 460	4 962	13 430	14 270	6.76
Limestone (Indiana)	13 040	4 983	13 036	4 992	12 755	13 625	8.4
Sandstone (Beria)	12 694	5 059	12 693	5 061	12 525	13 025	6.5
Sandstone (Boise)	10 992	5 034	10 994	5 042	10 860	11 385	2.8
Limestone (Indiana)	10 957	4 341	10 934	4 401	10 840	12 600	11.7
Sandstone (Boise)	10 187	4 500	10 175	4 529	10 130	11 160	8.43
Chalk	8 918	4 417	8 892	4 469	9 310	9 825	2.81
Chalk	7 642	4 614	7 637	4 624	7 930	8 135	9.257
Sandstone (Boise)	7 683	3 550	...	...	...	...	$-0.001\,\rho$ (assumed)

[a]Values taken from Ref. 26.

[b]Data taken from Ref. 19.

The pole $s=\eta$ contributes another steady state solution of Eq. (8). On superimposing this solution with Eq. (12) the amplitude ratio of the subsequent cycles can be expressed as

$$\frac{A_1}{A_2}=\exp\left(\frac{-b(Q+R)}{Q\rho_{22}-R\rho_{12}}\Delta\tau\right), \tag{13}$$

where $\Delta\tau$ is the time period between A_1 and A_2. It can be shown that this amplitude ratio is nearly unity for the material constants used in this investigation.

The square root term in the denominator of the integral of Eq. (8), and the expressions of λ_1 and λ_2 when equated to zero separately contribute four branch points s_1, s_2, s_3, and s_4 as shown in Fig. 3. Thus the integration along the contour as depicted in Fig. 3 yields the following expression for displacement due to branch

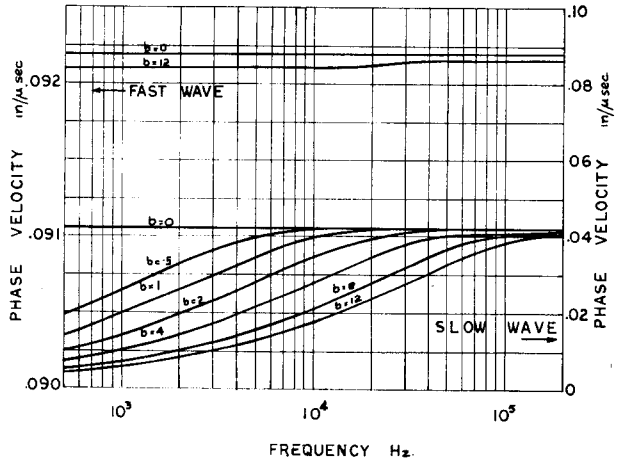

FIG. 5. Dispersion curves of waves in kerosene-saturated Boise sandstone.

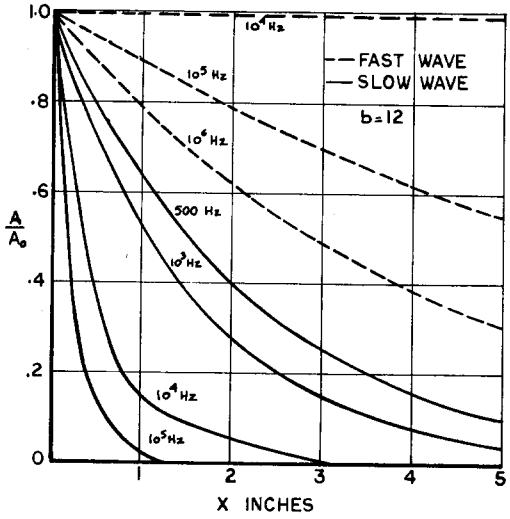

FIG. 7. Amplitude decay of the fast and slow waves in water-saturated Boise sandstone. Damping coefficient $b = 12$.

points alone:

$$u + U = \frac{mU_{in}\omega}{\pi}\left[\int_0^{S_4} \frac{[-ra - f - (r^2 - dr + f^2)^{1/2}][-rh - n + (r^2 - dr + f^2)^{1/2}]e^{-rt}\sin(r/2A)\{r[(D/C) - r]\}^{1/2}x}{(r^2 - dr + f^2)^{1/2}(r + \eta)(r^2 + \omega^2)}\,dr\right]. \quad (14)$$

Equation (14) contributes small oscillations superimposed on the initial portion of the main pulse. After considerable numerical evaluations, it can be shown that the contributions from Eq. (14) are small in comparison with the contributions from the poles in the cases discussed.

II. CONCLUSION AND DISCUSSION

From the wave analysis presented in the previous section, it can be concluded that the main bodies of the waves are two steady states waves due to the poles $s = \pm i\omega$. These two waves propagate with a constant velocity v_f and v_s [Eq. (11)] depending upon the material properties of the saturating fluid and the porous medium. The magnitude of these two velocities cannot, however, be readily calculated from Eq. (11) since the parameter ρ_{12}, which describes the interaction between the solid and the fluid portion of the medium, is unknown. Using the same experimental arrangement as sketched in Fig. 1, Gregory[22] and Wyllie[21] have made an extensive investigation on the wave speeds in the fluid-

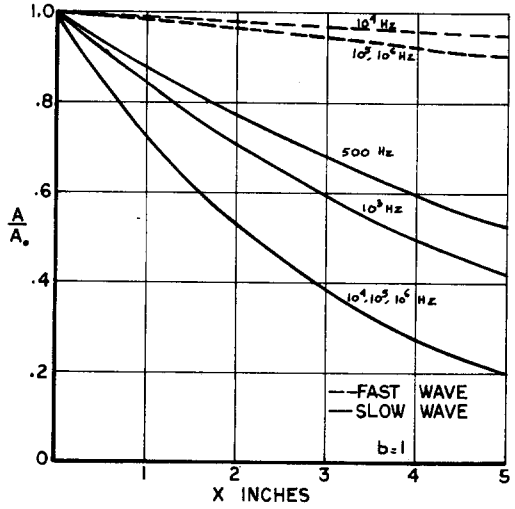

FIG. 6. Amplitude decay of the fast and slow waves in water-saturated Boise sandstone. Damping coefficient $b = 1$.

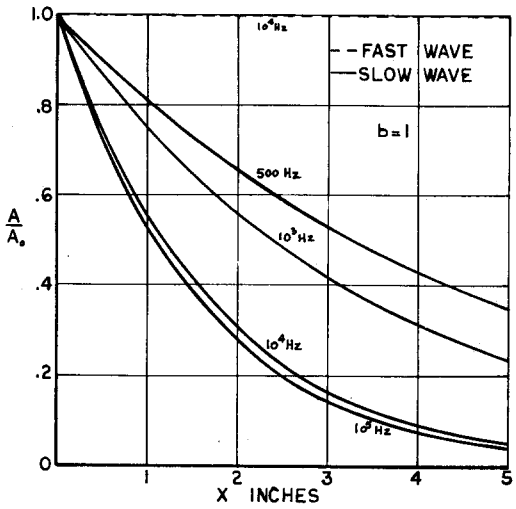

FIG. 8. Amplitude decay of fast and slow waves in kerosene-saturated Boise sandstone. Damping coefficient $b = 1$.

saturated rocks. For reasons that will be made clear in the later discussions, only the fast waves (i.e., waves traveling with speed v_f) were observed in the experiment (for an example, see Fig. 2). Using Gregory's data, the parameter ρ_{12} for rocks under various confining pressures is calculated and tabulated in Table I along with the wave speeds calculated by assuming $\rho_{12}=0$. It is clear that the magnitude of ρ_{12} is small and its contribution to the magnitude of wave speeds is approximately 13% at the most. It should however be mentioned here that some errors might have been involved in the determination of Biot's constants P, Q, and R. The method of determining these constants is presented in Appendix I. The small value of ρ_{12} implies that the interaction between the solid and fluid portions of the medium is not strong in this type of experiment. By letting $\rho_{12}=0$, Eq. (11) may be written as

$$V_{1,2}^2=\frac{2\alpha_s^2\alpha_f^2(1-Q^2/\rho_s\rho_f\alpha_f^2\alpha_s^2)}{[\alpha_f^2(1-\beta)+\alpha_s^2\beta]\mp([\alpha_f^2(1-\beta)-\alpha_s^2\beta]^2+4Q^2\beta(1-\beta)/\rho_s\rho_f)^{1/2}}\ , \tag{15}$$

where $\alpha_s=(P/\rho_s)^{1/2}$ and $\alpha_f=(R/\rho_f)^{1/2}$. If further assumptions are made that the terms $Q^2/\rho_s\rho_f\alpha_s^2\alpha_f^2$ and $4Q^2\beta(1-\beta)/\rho_s\rho_f$ were small in comparison with its other terms, an approximate formula for computing the fast and slow wave speeds can be written as

$$v_f^2=\alpha_s^2/(1-\beta)=P/\rho_s(1-\beta) \tag{16}$$

$$v_s^2=R/\rho_f\beta\ . \tag{17}$$

Since $P=2\mu+\lambda$, where λ and μ are the Lame constants for the porous medium, we conclude that the fast wave is equivalent to the dilatational wave when the porous material is modelled as a homogeneous elastic medium. The wave speeds calculated from Eqs. (16) and (17) are tabulated along with the measured wave speeds and those calculated from Eq. (11) in Table I. The results in general are in close agreement with each other.

The dispersive characteristics of both fast and slow waves are shown in Figs. 4 and 5. It is interesting to note that the fast wave shows very little dispersion. Furthermore, the dispersion of waves occurs only in a narrow frequency band (in the present case $10^3<\omega<2\times10^5$ Hz). This result agrees with the analytical predictions based on the mixture theory.[5] In the experimental investigation of wave motions in rocks, Podio[17] and Mousselli[25] also showed that the waves indeed exhibited very little dispersion. In contrast to the fast waves, the slow waves are highly dispersive. The phase velocity, nonetheless, reaches a constant value at high frequencies.

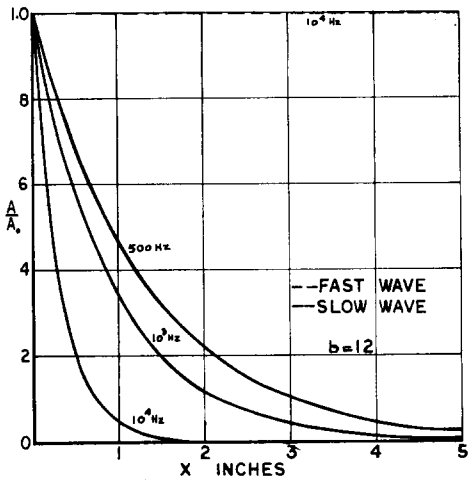

FIG. 9. Amplitude decay of fast and slow waves in kerosene-saturated Boise sandstone. Damping coefficient $b=12$.

The curves in Figs. 6–9 show the amplitude decrement of waves of both kinds with the distance at various frequencies for a damping factor $b=1$ and $b=12$. These curves clearly demonstrate that the rate at which the amplitude of slow waves decays is much faster than that of the fast waves. The amplitude of the slow wave decreases rapidly with the distance. Consequently it is difficult to be detected in practice unless a short specimen is used in the experiment. Based on this reason, and on the fact that the recorded waves showed no observable dispersions, we believe that the waves observed by Gregory,[23] Podio,[17] and Mousselli[25] were the fast waves. It is also interesting to note that the amplitude decrement of both waves is frequency dependent.

Based on the discussions presented in the above paragraphs, it seems evident that a great amount of information on the rock properties and damping effect of its contained fluid could be estimated by making a Fourier analysis of the measured fast wave generated by a wide-band pulse. A more accurate estimation could be achieved if the slow wave motion could be measured and analyzed along with the fast wave motion. The sonic-pulse technique, with the present arrangement, cannot generate a measurable slow wave. A remedial arrangement would be to replace the driving crystal with a device that could generate a high-intensity pulse. Another alternate means would be analyzing the shear wave motion along with the fast wave motion. These problems are currently being studied.

ACKNOWLEDGMENT

The authors wish to express their appreciation to Dr. A. R. Gregory for his interest and assistance during the course of investigation.

APPENDIX: DETERMINATION OF BIOT'S CONSTANTS

From Eq. (21) of Ref. 8, the Biot's constants P, Q, and R are defined as follows:

$$P=\lambda+2\mu, \tag{A1}$$

$$Q=\frac{\beta(1-\beta-\delta/k)}{\nu+\delta-\delta^2/k}\ , \tag{A2}$$

$$R=\frac{\beta^2}{\nu+\delta-\delta^2/k}\ , \tag{A3}$$

$$\lambda = \frac{\nu/k + \beta^2 + (1-2\beta)(1-\delta/k)}{\nu + \delta - \delta^2/k} - \frac{2}{3}\mu, \tag{A4}$$

$$\nu = \beta(C - \delta), \tag{A5}$$

where

β = porosity

μ = shear modulus of the bulk material,

k = coefficient of the jacketed compressibility,

δ = coefficient of the unjacketed compressibility,

C = compressibility of the fluid,

ν = coefficient of fluid content.

The constants k, δ, C are not given directly in Ref. 22. In this investigation, these constants are computed by using the following method:

(1) k = (the bulk modulus of the dry specimen under specified confining pressure)$^{-1}$

(2) δ = (the bulk modulus of a fully saturated specimen under specified confining pressure)$^{-1}$.

Both bulk moduli are determined from the measured wave speed in Ref. 22 and C is obtained from Ref. 26.

*This work is financially supported by the Bureau of Engineering Research at The University of Texas at Austin.

[1]C. W. Kosten and C. Zwikker, *Sound Absorbing Materials* (Elsevier, New York, 1949).
[2]R. W. Morse, "Acoustic Wave Propagation in Granular Media," J. Acoust. Soc. Am. 24, 696–700 (1956).
[3]N. R. Paterson, "Seismic Wave Propagation in Porous Granular Media," Geophysics 21, 691–714 (1956).
[4]A. Bedford and J. E. Ingram, "A Continuum Theory of Fluid Saturated Porous Media," J. Appl. Mech. 38, 1–7 (1971).
[5]L. Hsieh and C. H. Yew, "Wave Motions in a Fluid Saturated Porous Medium," J. Appl. Mech. 40, 657–661 (1973).
[6]M. A. Biot, "General Theory of Three Dimensional Consolidation," J. Appl. Phys. 12, 155–161 (1941).
[7]M. A. Biot, "Theory of Propagation of Elastic Wave in a Fluid Saturated Porous Solid: Part I and Part II," J. Acoust. Soc. Am. 28, 168–191 (1956).
[8]M. A. Biot and D. B. Willis, "The Elastic Coefficients of the Theory of Consolidation," J. Appl. Mech. 14, 594–962 (1961).
[9]J. P. Jones, "Rayleigh Waves in a Porous Elastic Fluid Saturated Solid," J. Acoust. Soc. Am. 33, 959–962 (1961).
[10]H. Deresiewicz, "The Effect of Boundaries on Wave Propagation in a Fluid Filled Porous Solid: Part I, Reflection of Plane Waves at Free Boundary (nondissipative case)," Bull. Seismol. Soc. Am. 50, 599–607 (1960).
[11]H. Deresiewicz, "The Effect of Boundaries on Wave Propagation in a Liquid Filled Porous Solid: Part II, Love Waves in a Porous Layer," Bull. Seismol. Soc. Am. 51, 51–59 (1961).
[12]H. Deresiewicz, "The Effect of Boundaries on Wave Propagation in a Liquid Filled Porous Solid: Part III, Reflection of Plane Waves at Free Plane Boundary (general case)," Bull. Seismol. Soc. Am. 52, 595–626 (1962).
[13]H. Deresiewicz, "The Effect of Boundaries on Wave Propagation in a Liquid Filled Porous Solid: Part IV, Surface Waves in a Half Space," Bull. Seismol. Soc. Am. 52, 627–638 (1962).
[14]J. Geertma and D. C. Smit, "Some Aspect of Elastic Wave Propagation in Fluid Saturated Porous Solid," Geophysics 26, 169–181 (1961).
[15]H. J. McSkimin, "Notes and References for the Measurement of Elastic Modulii by Means of Ultrasonic Waves," J. Acoust. Soc. Am. 33, 606–615 (1961).
[16]S. J. Pirson, *Handbook of Well Log Analysis* (Prentice–Hall, Englewood Cliffs, NJ, 1963).
[17]A. L. Podio, A. R. Gregory, and K. E. Gray, "Dynamic Properties of Dry and Water-Saturated Green River Shale Under Stress," J. Soc. Pet. Eng. 8, 389–404 (1968).
[18]G. H. Gardner, M. R. Wyllie, and D. M. Droschak, "Effect of Pressure and Fluid Saturation on the Attenuation of Elastic Waves in Sands," J. Pet. Technol. 16, 57–70 (1964).
[19]I. Fatt, "The Biot–Willis Elastic Coefficients for Sandstone," J. Appl. Mech. 26, 296–297 (1959).
[20]M. R. Wyllie, A. R. Gregory, and G. H. Gardner, "Elastic Wave Velocity in Heterogeneous and Porous Media," Geophysics XXI, 41–70 (1956).
[21]M. R. Wyllier, A. R. Gregory and G. H. Gardner, "An Experimental Investigation of Factors Affecting Elastic Wave Velocities in Porous Media," Geophysics XXIII, 459–493 (1958).
[22]A. R. Gregory, "Fluid Saturation Effects on Dynamic Elastic Properties of Sedimentary Rocks" (private communication).
[23]A. R. Gregory and A. L. Podio, "Dual-Mode Ultrasonic Apparatus for Measuring Compressional and Shear Wave Velocities of Rock Samples," IEEE Trans. Sonics Ultrason. SU-17, 77–85 (1965).
[24]C. H. Yew and P. N. Jogi, "A Study of Wave Motions in Fiber-Reinforced Medium," Int. J. Solids Struct. (to be published).
[25]A. Mousselli, "Experimental Investigation of Stress Wave Attenuation in Gas-Saturated Rocks," Ph. D. dissertation (University of Texas at Austin, 1974) (unpublished).
[26]C. Carmichael, *Kent's Mechanical Engineer's Handbook*, 12th ed. (Wiley, New York, 1965).